DISCONTINUOUS SEISMIC HORIZON TRACKING BASED ON A POISSON EQUATION WITH INCREMENTAL DIRICHLET BOUNDARY CONDITIONS

G. Zinck, M. Donias*, S. Guillon** and O. Lavialle**

* Université de Bordeaux, IPB, Laboratoire IMS CNRS UMR 5218, 351 cours de la Libération, 33405 Talence cedex, France.
** TOTAL CSTJF, Avenue Larribau, 64018 Pau, France.
[guillaume.zinck marc.donias olivier.lavialle]@ims-bordeaux.fr,
sebastien.guillon@total.com

ABSTRACT

We propose a new method to track a seismic horizon with a discontinuity due to a fault throw assumed to be quasi-vertical. Our approach requires the knowledge of the two points delimiting the horizon as well as the discontinuity location and jump. We deal with a non linear partial derivative equation relied on the estimated local dip. Its iterative resolution is based on a Poisson equation with incremental Dirichlet boundary conditions. By exploiting a coherence criterion, we finally present an efficient method even when the discontinuity location and jump are unknown.

Index Terms— Seismic horizon tracking, Poisson equation, Incremental boundary conditions, Fault detection.

1. INTRODUCTION

Manual seismic data interpretation is a difficult and time-consuming task. That is why many recent numerical frameworks have been dedicated to understanding geological processes [1]. In this paper, we particularly focus on tracking seismic horizons [2][3]. Some authors [4][5] consider a non linear partial derivative equation (PDE) relied on the estimated local dip. Lomask *et al.* [5] propose to solve it with a global optimization technique using an iterative algorithm. Unfortunately, this approach only achieves for continuous horizons. Assuming that a discontinuity arises from a quasi-vertical fault throw, we present a new PDE approach capable of tracking a discontinuous horizon. The method is based on a linear Poisson equation with incremental boundary values.

2. HORIZON TRACKING ALGORITHM

A seismic horizon can be considered as a curved segment represented by a function τ defined between two abscises x_1 and x_2. The function (figure 1a) is supposed to be discontinuous at abscise $\alpha \in]x_1, x_2[$ with a jump $C_c = \lim_{x \to \alpha^+} \tau(x) - \lim_{x \to \alpha^-} \tau(x)$.

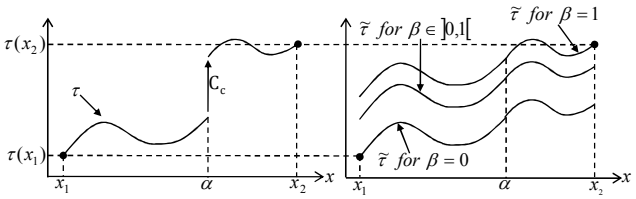

Figure 1a - Discontinuous seismic horizon.
Figure 1b - Influence of the value of β on the function $\tilde{\tau}$.

The tracking of a continuous horizon is obtained by solving a PDE that connects τ to the tangent p of the local dip:

$$\forall x \in [x_1, x_2], \ \nabla\tau(x) = p\big(x, \tau(x)\big), \qquad (1)$$

where ∇ denotes the gradient operator [5]. The local dip, which corresponds to the angle between the horizon and the horizontal axis, is a known dense field previously estimated over the entire seismic image. Its tangent p and τ are respectively considered as functions of class C^1 and C^2. When the tracked horizon is discontinuous, τ is a function of class C^2 only on $[x_1, x_2] - \{\alpha\}$. We propose to decompose it into the sum of an unknown C^2 class function on $[x_1, x_2]$ denoted $\tilde{\tau}$ and a discontinuous function $\hat{\tau}$. The function $\tilde{\tau}$ is obtained by solving equation:

$$\forall x \in [x_1, x_2], \ \nabla\tilde{\tau}\,(x) = p\big(x, \tilde{\tau}(x) + \hat{\tau}(x)\big), \qquad (2)$$

while $\hat{\tau}$ is defined by:

$$\hat{\tau}(x) = -\beta C_c \mathrm{H}(\alpha - x) + (1-\beta) C_c \mathrm{H}(x - \alpha), \qquad (3)$$

where β is chosen between 0 and 1 and H is the Heaviside step function:

$$\mathrm{H}(x) = \begin{cases} 0 \text{ if } x \leq 0 \\ 1 \text{ if } x > 0 \end{cases}. \qquad (4)$$

The value of β impacts the mean value of $\tilde{\tau}$ by partially matching τ and $\tilde{\tau}$ either on the left side ($\beta = 0$) or on the right side ($\beta = 1$) of the discontinuity (figure 1b). Any intermediate value of $\tilde{\tau}$ is obtained for β in]0,1[. Equation (2) is non linear because p depends on τ, thus an iterative algorithm is used to get $\tilde{\tau}$.

2.1. Solution in continuous domain

The algorithm consists of an initialization step, an iterative step and a final step. $\tilde{\tau}$ is initialized to a constant reference $y_r \in [\tau(x_1), \tau(x_2)]$ controlled by β. The iterative step is made of three parts: residual computation, update term computation and updating. As described in the previous section, τ is finally computed as the sum of the calculated function $\tilde{\tau}$ and $\hat{\tau}$.

Initialization step:

$$\begin{gathered} \forall x \in [x_1, x_2], \\ \tilde{\tau}_0(x) = y_r = \tau(x_1) + \beta\big(\tau(x_2) - \tau(x_1)\big). \end{gathered} \tag{5}$$

Iterative step:

- *Residual computation:*

$$r_k(x) = \nabla\tilde{\tau}_k(x) - p\big(x, \tilde{\tau}_k(x) + \hat{\tau}(x)\big). \tag{6}$$

- *Update term computation:*

$$\Delta(\delta\tilde{\tau}_k) = -\mathrm{div}(r_k), \tag{7}$$

where Δ denotes the Laplace operator and div is the divergence vector operator. Equation (7) is a Poisson equation associated with two boundary values $\delta\tilde{\tau}_k(x_1)$ and $\delta\tilde{\tau}_k(x_2)$ called Dirichlet conditions which ensure the unicity of the solution:

$$\begin{gathered} \begin{cases} \delta\tilde{\tau}_0(x_1) = -\beta(\tau(x_2) - \tau(x_1) - C_c) \\ \delta\tilde{\tau}_0(x_2) = (1-\beta)(\tau(x_2) - \tau(x_1) - C_c) \end{cases} \\ \text{and } \begin{cases} \delta\tilde{\tau}_k(x_1) = 0 \\ \delta\tilde{\tau}_k(x_2) = 0 \end{cases} \forall k > 0. \end{gathered} \tag{8}$$

- *Updating:*

$$\tilde{\tau}_{k+1}(x) = \tilde{\tau}_k(x) + \delta\tilde{\tau}_k(x). \tag{9}$$

According to equation (8), the boundaries of $\tilde{\tau}$ are fixed after the first iteration. Convergence is assumed to be reached after a number K of iterations.

Final step:

$$\tau(x) = \tilde{\tau}_K(x) + \hat{\tau}(x). \tag{10}$$

2.2. Solution in discrete domain

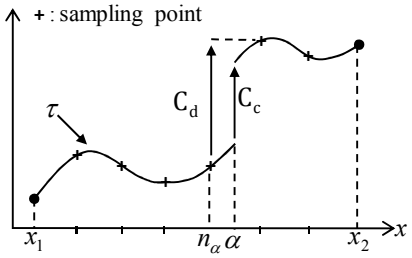

Figure 2 - Continuous and discrete jump.

In a numerical solving of equation (2), the interval $[x_1, x_2]$ is sampled in N points. As the discontinuity location α is not necessary a sampling point, let n_α denote the index $\epsilon\,[1, N]$ of the largest sampling point value that is not greater than α. The notion of continuous jump is irrelevant (figure 2), so C_c is replaced by a discrete jump $C_d = \tau(n_\alpha + 1) - \tau(n_\alpha)$. Introducing C_d in the Dirichlet boundary conditions implies that the boundaries of $\tilde{\tau}$ cannot be fixed after one iteration because $\delta\tilde{\tau}(n_\alpha) \neq \delta\tilde{\tau}(n_\alpha + 1)$. As a result, the previous algorithm is modified by adding incremental Dirichlet boundary conditions relied on a jump C initialized to C_d and updated at each iteration. The discontinuous function $\hat{\tau}$ is consequently updated too.

Initialization step:

$$\begin{gathered} \forall\, n \in [1, N], \quad \tilde{\tau}_0(n) = y_r \\ C_0 = C_d \\ \hat{\tau}_0(n) = -\beta C_0 \mathrm{H}(n_\alpha + 1 - n) + \\ (1-\beta) C_0 \mathrm{H}(n - n_\alpha). \end{gathered} \tag{11}$$

Iterative step:

- *Residual computation:*

$$r_k(n) = \nabla\tilde{\tau}_k(n) - p\big(n, \tilde{\tau}_k(n) + \hat{\tau}_k(n)\big) \tag{12}$$

- *Update term computation:*

$$\Delta(\delta\tilde{\tau}_k) = -\mathrm{div}(r_k) \tag{7}$$

with the following Dirichlet conditions:

$$\begin{gathered} \begin{cases} \delta\tilde{\tau}_0(1) = -\beta(\tau(x_2) - \tau(x_1) - C_0) \\ \delta\tilde{\tau}_0(N) = (1-\beta)(\tau(x_2) - \tau(x_1) - C_0) \end{cases} \\ \text{and } \begin{cases} \delta\tilde{\tau}_k(1) = -\beta(C_{k-1} - C_k) \\ \delta\tilde{\tau}_k(N) = (1-\beta)(C_{k-1} - C_k) \end{cases} \forall k > 0. \end{gathered} \tag{13}$$

- *Updating:*

$$\begin{gathered} \tilde{\tau}_{k+1}(n) = \tilde{\tau}_k(n) + \delta\tilde{\tau}_k(n) \\ C_{k+1} = C_d - \big(\tilde{\tau}_{k+1}(n_\alpha + 1) - \tilde{\tau}_{k+1}(n_\alpha)\big) \\ \hat{\tau}_{k+1}(n) = -\beta C_{k+1} \mathrm{H}(n_\alpha + 1 - n) \\ + (1-\beta) C_{k+1} \mathrm{H}(n - n_\alpha). \end{gathered} \tag{14}$$

It can be noted that the difference $C_{k-1} - C_k$ converge to 0, which guarantees the convergence of the algorithm.

Final step:

$$\tau(n) = \tilde{\tau}_K(n) + \hat{\tau}_K(n). \tag{15}$$

Equation (7) is solved [6][7] by a direct Fourier transform method:

$$\delta\tilde{\tau}_k = \mathrm{DFT}^{-1}\left[\frac{\mathrm{DFT}[-\mathrm{div}(r_k)]}{\mathrm{DFT}[\Delta]}\right], \tag{16}$$

where DFT and DFT^{-1} are respectively the discrete Fourier transform and the inverse discrete Fourier transform. The ability to invert the Laplace operator is described in [6]. Using DFT implicitly assumes that the input sequence is periodic, thus an odd mirror is applied to check the boundary values and avoid undesirable effects [7]. A type-I Discrete Sine Transform (DST) can then be employed to compute each transform in $\mathcal{O}(N\log N)$time.

3. DISCONTINUITY DETECTION METHOD

Assuming that an horizon presents a discontinuity with an unknown jump C_d at an unknown location n_α, its tracking can be obtained by testing several candidates (n_α, C_d) and identifying the optimal one $\left(n_\alpha^{opt}, C_d^{opt}\right)$.

A naïve and calculation time-consuming method is an exhaustive test by taking n_α and C_d in chosen sampled intervals. Various coherence criteria can then be used to find $\left(n_\alpha^{opt}, C_d^{opt}\right)$. The attribute presented in [8] measures the correlation level between vertical traces within a small analysis window neighborhood. The gradient disorder criterion described in [9] performs the two-dimensional coherence of the gradient vector. Donias *et al.* [10][11] address a fault attribute based on a robust directional scheme. This method is well-suited to differentiate faults from stratigraphic features and consists in performing an eigenstructure analysis of the gradient vector field covariance matrix along a segment. We establish the gradient on L sampled points along the segment $\boldsymbol{u} = \left[\left(n_\alpha, \tau(n_\alpha)\right), \left(n_\alpha + 1, \tau(n_\alpha + 1)\right)\right]$. The coherence criterion computed for the candidates (n_α, C_d) is defined by:

$$c(n_\alpha, C_d) = \frac{\lambda_1 - \lambda_2}{\lambda_1 + \lambda_2}, \tag{17}$$

where λ_1 and λ_2 are the eigenvalues in decreasing order of the approximated covariance matrix. Eigenvalues are very close on a fault, leading to an attribute close to zero. In contrast, the largest eigenvalue λ_1 is much higher than the other one and the criterion tends to 1 in the absence of fault.

Owing to the criterion sensitivity to all stratigraphic signatures, the global minimum of the criterion response calculated for all candidates (n_α, C_d) can sometimes be an irrelevant peak and does not correspond to the optimal horizon. For a given n_α, the mean $\bar{c}$ of the coherence attributes for all tested jumps is therefore calculated to reduce influence of irrelevant peaks. The optimal location n_α^{opt} is the argument of this mean criterion minimum. The optimal jump stems from a dispersion measure on the tested horizon:

$$C_d^{opt} = \arg\min_{C_d} \sigma_s, \tag{18}$$

where s is the seismic amplitude along the horizon τ and σ its standard deviation.

4. RESULTS AND DISCUSSIONS

4.1. Synthetic data

The horizon tracking algorithm is firstly tested on a synthetic image obtained from a mathematic model τ_{th} corrupted by an additive two-component Gaussian mixture (figure 3). The discontinuity location and jump are assumed to be known. Figure 4 depicts the difference D between the estimated function τ and τ_{th} for 1, 2 and 10 iterations.

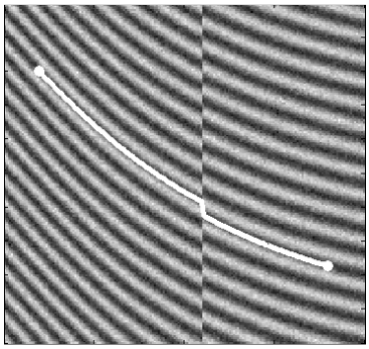

Figure 3 - Noisy synthetic image (200 × 200) with the tracked horizon for $C_d = 8.2$ and $n_\alpha = 110$.

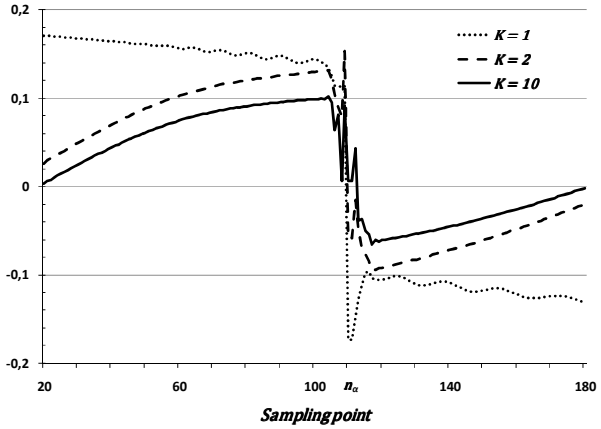

Figure 4 - $D = \tau - \tau_{th}$ for different values of K.

In the area around the discontinuity, the difference D is extremely weak (less than 0.2 pixels for one iteration). On the boundary, D is insignificant and tends towards zero (10^{-3} for 10 iterations, 10^{-4} for 30 iterations). That proves precision, fast convergence and noise robustness of our algorithm.

4.2. Real seismic data

The horizon tracking algorithm is also validated on numerous real seismic data for which the fault location and jump are unknown. Figure 5 shows an example of a seismic data with two input points. The candidates n_α and C_d are

chosen respectively in the sampled interval $[x_1 + 1, x_2 - 1]$ and $[-17, -2]$ with a 0.5 step while $L = 10$ points are taken on $\boldsymbol{u}$.

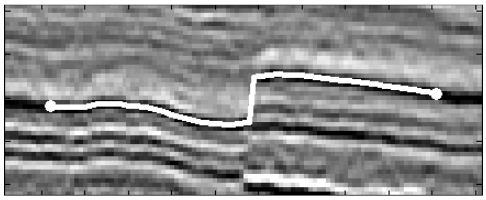

Figure 5 - Seismic data with two input points and the optimal tracked horizon.

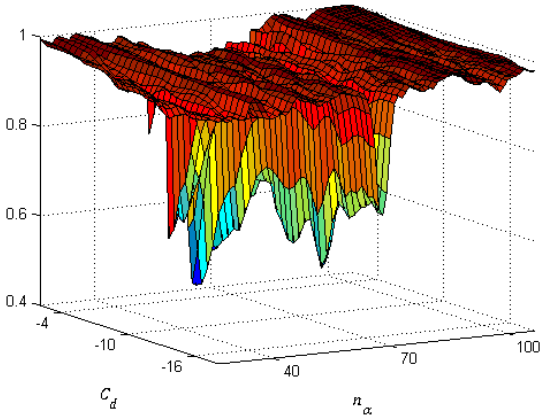

Figure 6 - Coherence criterion response.

Figure 6 presents the coherence criterion response. A meaningful line of local minimum values corresponds to a given fault location n_α. Irrelevant peaks nevertheless appear due to the criterion sensitivity to other stratigraphic features. Increasing the value of L slightly affects the results by smoothing the response without eliminating artifacts. Computing the mean $\bar{c}$ of the coherence attribute for each value of n_α (figure 7a) provides an extremely discriminatory criterion to detect the fault location. This criterion proves the significant accuracy of our method. Once n_α^{opt} is fixed, the dispersion measure defined in equation (18) offers a proper estimation of the fault jump (figure 7b).

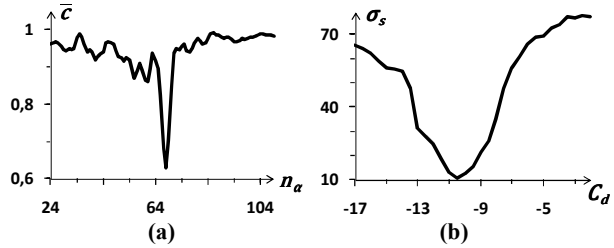

Figure 7a – Mean of the coherence attribute.
Figure 7b - Standard deviation of the seismic amplitude along the tested horizons.

Figure 5 also depicts the optimal tracked horizon for 30 iterations. Discontinuity location and jump are well predicted and the identified horizon seems to be merged with the observable one.

5. CONCLUSION

We have developed a new algorithm to track a seismic horizon with a quasi-vertical discontinuity. Only the knowledge of the two points delimiting the horizon and the estimated local dip are required. Our approach consists in an iterative global optimization technique when the key point is a Poisson equation with incremental Dirichlet boundary conditions. The obtained results exhibit good performances on both synthetic and real data.

6. ACKNOWLEDGMENTS

The authors thank Total company for supporting this work and supplying seismic data.

7. REFERENCES

[1] Donias, M., Guillon, S., Baylou, P., Pauget, F., and Keskes, N., "Method of chrono-stratigraphic interpretation of a seismic cross section or block", Elf Exploration Production, U.S. Patent N° 2001/0036294, Nov. 1, 2001.

[2] Benbernou, R., and Warwick, K., "A fuzzy multicriteria decision approach for enhanced autotracking of seismic events", International Conference on Signal Processing and Communications, pp. 1331-1334, 2007.

[3] Gallon, J., Guillon, S., Jobard, B., Barucq, H. and Keskes, N., "Slimming brick cache strategies for seismic horizon propagation algorithms", International Symposium on Volume Graphics, pp. 37-44, 2010.

[4] Bienati, N., and Spagnolini, U., "Traveltime picking in 3D data volumes", 60th European Association of Geoscientists & Engineers Meeting, 1998.

[5] Lomask, J., Guitton, A., Fomel, S., Claerbout, J., and Valenciano, A., "Flattening without picking", *Geophysics*, Vol. 71, No. 4, pp. 13-20, 2006.

[6] Strang, G., "Introduction to applied mathematics", *Wellesley-Cambridge Press*, 1986.

[7] Bhat, P., Curless, B., Cohen, M., and Lawrence Zitnick, C., "Fourier analysis of the 2D screened Poisson equation for gradient domain problems", European Conference on Computer Vision, pp. 114-128, 2008.

[8] Gersztenkorn, A., and Marfurt, K. J., "Eigenstructurebased coherence computations as an aid to 3-D structural and stratigraphic mapping", *Geophysics*, Vol. 64, No. 5, pp. 1468-1479, 1999.

[9] Randen, T., Mosen, E., Signer, C., Abrahamsen, A., Hansen, J.O., Saeter, T., Schlaf, J., and Sonneland, A., "Three-dimensional texture attributes for seismic data analysis", 70th Internat. Mtg., Soc. Expl. Geophysics, Expanded Abstracts, pp. 668-671, 2000.

[10] Donias, M., David, C., Lavialle, O., Berthoumieu, Y., Guillon, S., and Keskes, N., "New fault attribute based on a robust directional scheme", *Geophysics*, Vol. 72, No. 4, pp. 39-46, 2007.

[11] Berthoumieu, Y., Donias, M., Guillon, S., and Keskes, N., "Extraction de plans de fracture dans un bloc sismique", European Patent N° 5906898, 2005.